Appeared in the Proc. of the First IEEE International Conference on Biometrics: Theory, Applications and Systems (BTAS), (Washington DC, USA), September 2007

Extended Evaluation of Simulated Wavefront Coding Technology in Iris Recognition

Kelly N. Smith, V. Paul Pauca, Arun Ross, Todd Torgersen, Michael C. King*

***Abstract*—The iris is a popular biometric that has been demonstrated to exhibit high matching accuracy and permanence under appropriate conditions. However, there are several limiting factors that are yet to be comprehensively addressed. One major drawback, in standard limited-focus iris recognition systems, is the restrictions imposed by the optical parameters of the acquisition system on the depth of field. Recently, wavefront coding technology has been proposed as a method to extend the depth of field of such limited-focus imaging systems. In this work we examine the utilization of a *simulated* wavefront coded element for increasing the operational range of iris recognition, without affecting the computational requirements of the system. A statistically relevant dataset of 150 iris images from 50 subjects is employed in a simulation study to determine the matching performance of a standard limited-focus system and a wavefront coded iris imaging system over an extended depth of field. It is shown that the operational range for iris recognition can be significantly increased, without the need to post-process the wavefront coded imagery.**

I. Introduction

A major limitation of standard limited-focus iris recognition systems [1][2][18] is the inability to obtain an in-focus image of the iris at varying distances. In order to obtain an in-focus image, the object must be within the volume of the depth of field, a characteristic that is heavily dependent on the system optics. Often times, iris biometric users are forced to "play the trombone" in order to present their iris within this imaging volume. **Fig. 1** illustrates the concept of an imaging volume applied to a typical iris recognition scenario, where a user must submit a sample of his iris to the acquisition system, to gain access to a secure environment. The shaded box indicates the imaging volume that will produce an in-focus acceptable image for processing.

Because the iris is a moving object residing on two independently moving objects (the human eye and the human), emphasis is also placed on capturing an image *quickly* to alleviate the effects of motion blur. Dealing with these constraints is an important consideration when designing or selecting an iris capture device. A closer look at some relevant basic optics parameters will help one appreciate the tradeoffs associated with these various choices.

* Smith and King are with the Intelligence Technology Innovation Center (ITIC). Pauca and Torgersen are with Wake Forest University. Ross is with West Virginia University.

A. Optical Parameters

Variations in optical system characteristics, such as focal length and pupil diameter, can greatly affect the results of an imaging system, even when the same lens is used. For example, the f number, f|#, i.e. the ratio of the effective focal

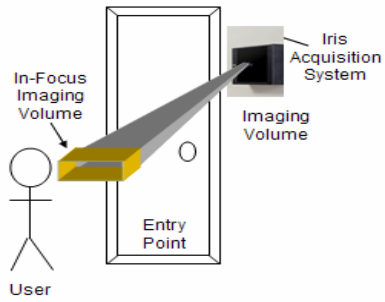

Fig. 1. Iris recognition imaging volume

length of the lens to the diameter of the entrance pupil [3], has a large effect on the depth of field. Increasing the f|# increases the depth of field, at the expense of loss of optical flux reaching the image plane. Decreasing the aperture size results in under-exposed, low contrast, and noise dominated low-quality images. It can also worsen the diffraction limited resolution at the in-focus plane. This effect cannot be easily mitigated by a system attempting to capture a high quality iris image. Any attempt to increase the depth of field by stopping down the aperture will invariably require increased exposure times which can lead to degradations due to motion blur.

B. Extending the Depth of Field via Wavefront Coding

Wavefront coding (WFC) is a novel imaging modality, where a unique aperture configuration is used to increase the depth of field, without significantly decreasing the signal to noise ratio (SNR) [4]. This approach, originally proposed by Dowski and Cathey [4], is a computational or task-based imaging technique where an image is deliberately distorted by a known amount but in a way that is insensitive to misfocus blur. Although not necessarily visually pleasing, the distorted image encodes depth dependent intensity information, which can be digitally recovered for sufficient SNR, leading to an increased depth of field. More specifically, wavefront coding places a separable cubic phase mask of the form,

$$\phi(x, y) = \alpha(x^3 + y^3) \quad (1)$$

in the pupil of a standard limited-focus imaging system to encode a 3-dimensional scene so as to produce an intermediate image with a nearly spatially invariant blur

corresponding to a known point spread function. Here the x and y coordinates are in the pupil plane, and the multiplier α determines the overall strength of the mask [5]. Signal processing may then be employed to digitally restore the intermediate image via a decoding operation. Fig. 2 illustrates the difference between conventional limited-focus and wavefront coded systems.

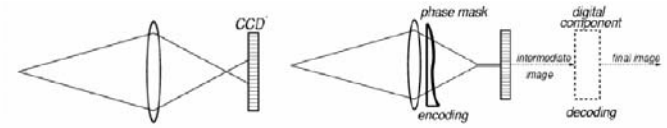

Fig. 2. Standard (left) and cubic phase (right) imaging systems [5].

The introduction of a cubic phase mask in the system pupil plane can yield a large amount of focus invariance in the modulation transfer function (MTF) over an extended imaging volume, at the cost of a decrease in the signal to noise ratio [6][8][9]. Under appropriate conditions, the cubic MTF typically does not contain nulls seen in the MTF of conventional imaging systems as defocus distance increases [6][13][14]. The information loss associated with nulls in the MTF seen in conventional imaging systems, results in a significant degradation in the performance of iris recognition algorithms that no amount of post processing can recover.

Since its original proposal, wavefront coding has been extended to include more general separable and non-separable type surfaces or phase masks [7][8][9][10]. A more recent development includes a novel general framework, known as pupil phase engineering (PPE), to address high quality image acquisition from a numerical optimization perspective [11][12]. In this framework, image quality requirements may include extending the depth of field, controlling or minimizing the impact of aberrations, motion blur, scattering from the imaging medium, among others (see, e.g., [12] and references therein).

TABLE I
OPERATIONAL RANGE FOR IRIS RECOGNITION OF A STANDARD SYSTEM AND A WFC IMAGING SYSTEM [5].

Image Type	Distance Range (cm)		Operational Range (cm)
Standard	-7	7	~14
Wavefront Coded	-10	13	~23

The use of phase masks in iris recognition imaging systems is a promising approach that could greatly extend the operational range of iris recognition [5][6][15], thereby facilitating flexibility when a user interacts with the system. One limitation of the published work [9][15] is the small dataset size (<10 user irises) over which wavefront encoding has been evaluated (see also Table 1). The present work examines the use of *unrestored* (intermediate) wavefront encoded imagery for extending the operational range of iris recognition on a larger dataset of 150 iris images pertaining to 50 subjects. The use of unrestored imagery is based on the premise that wavefront encoding can expose sufficient low and mid frequency information in the MTF to enable successful iris recognition over an extended distance. The use of *restored* wavefront coded imagery will be examined in future work.

The rest of the paper is organized as follows. In section II we describe the dataset, methods, and tools employed to generate and evaluate the simulated wavefront coded imagery. In section III we present Hamming distance results related to the recognition performance of conventional and wavefront coded imaging systems. Finally, concluding remarks and future work are stated in section IV.

II. Data Simulation

A. Dataset

In order to increase the size of the dataset, reliable data from a diverse population needed to be used. The authors acquired the images used in this study from the Iris Challenge Evaluation (ICE) dataset [14][1]. Images were hand selected to ensure in-focus frontal images with few occlusions. This effort was required to minimize the presence of confounding factors known to affect iris recognition performance, thereby ensuring that the observed matching results were a consequence of the cubic phase element, rather than other variables. Fifty (50) users were selected, each represented by three (3) different images. **Fig. 3** shows a subset of the data. The selected 150 in-focus iris images were used as ground truth in our study as well as to generate all the simulated intermediate conventional out-of-focus blurred and wavefront encoded imagery.

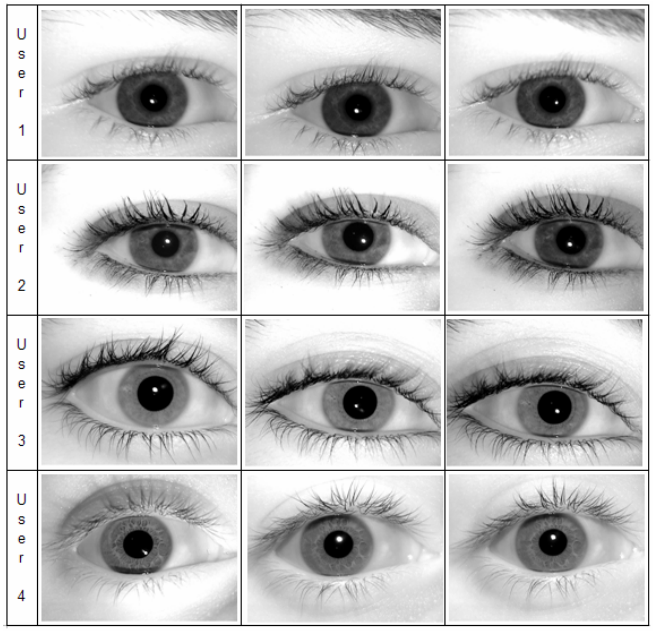

Fig. 3. Sample images from the ICE dataset [16].

B. Simulation Tool

For a single-lens incoherent imaging system and an object

[1] For information on the selected ICE images, contact author K. Smith.

placed at a uniform distance from the imaging device, the image formation process is typically modeled as a convolution of the form

$$g = h \otimes f + \eta \,, \tag{2}$$

where f is the input signal, η describes a noise process, h is the system point spread function (PSF), and g is the resulting blurred and noisy image. The PSF h is given by:

$$h = \left| F\left\{ P(x,y)\exp(i(\tau(x^2+y^2)+\phi(x,y)) \right\} \right|^2 . \tag{3}$$

Here $P(x,y)$ is the system pupil function equal to 1 for all x inside the pupil and 0 outside, and τ is the defocus parameter. We adopt a widely-used noise model [19] given by:

$$\eta = \sqrt{h \otimes f}\,\eta_1 + \sigma\eta_2 . \tag{4}$$

Both η_1 and η_2 are standard normally distributed zero-mean random variables with variance equal to one. The parameter σ is the standard deviation of the image-independent noise term. The first term in equation (4) approximates the Poisson noise associated with the light detection process.

A software tool known as Simulator of Iris Recognition Imaging Systems (SIRIS) was used to generate the blurred standard and wavefront encoded images. SIRIS is a Matlab-based system developed by Wake Forest University researchers[2] that includes the image formation, PSF, and noise models of equations (2-4) to explore the performance of separable and non-separable phase masks on iris recognition [17]. Among other functionalities, SIRIS also allows the user to specify optical characteristics and parameters of an imaging device. These parameters can include focal length, object distance, pupil diameter, pixel pitch and noise. **Fig. 4** is a screen shot of the SIRIS front-end [17].

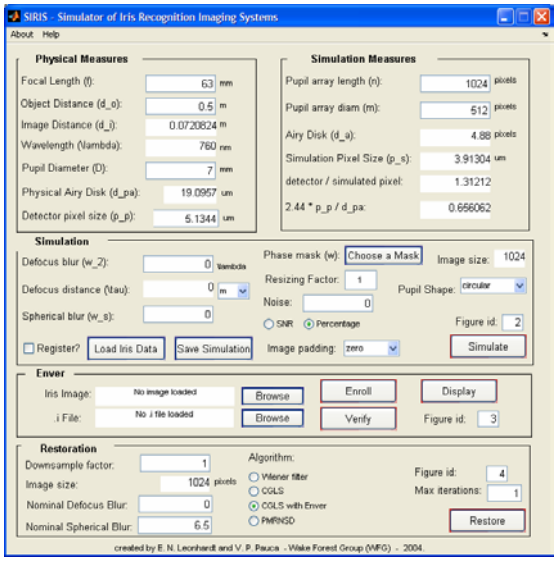

Fig. 4. A screen-shot of the SIRIS simulation tool.

Using the specified optical and detector parameters as well as the input imagery, SIRIS generates corresponding output images that include the effects of a pre-specified phase mask and noise characteristics. The software system also provides the waves of defocus blur corresponding to any specific distance from the plane of best focus. The result is a model that summarizes the effects of defocus blur and the phase mask on the imaging system. Parameters were selected based on the optical characteristics of the system used to collect the ICE images, viz., the LG2200 at Notre Dame University [16]. Table II lists some of the parameters that were used as input values to SIRIS.

TABLE II
PARAMETERS COMPUTED FOR INPUT TO SIRIS

Parameter	Value
Focal Length	53mm
Object Distance	0.5m
Pupil Diameter	27.5mm
Detector Pixel Size	5.134μm

C. *Pupil Phase Mask Selection*

For this study, a cubic phase element with α=30 (see equation (1)) was employed. The intention was to simulate the effects of a pupil phase mask consistent with the one used in previous work. Other phase masks, such as the higher order PPE mask designs, may also be evaluated. Other parameters were selected based on the published literature [5]. Simulation results were first verified visually by collaborators at CDM Optics.

D. *Simulated Images*

The standard deviation σ for the noise independent component was set to 0.01 (1% noise), and characterizes a camera under ideal lighting and image capture conditions. Two types of blurred images were simulated for this study.

- Standard Images: The set of standard images are affected by varying amounts of defocus blur τ due to movement of the iris away and towards the imaging device. This distance ranged from -10.2cm (away) to 10.2 cm (towards) from the plane of best focus. This range was selected because it was significantly wider than the known imaging volume of the standard system. See Fig. 5 for a sample set of blurred images based on a single input image f.

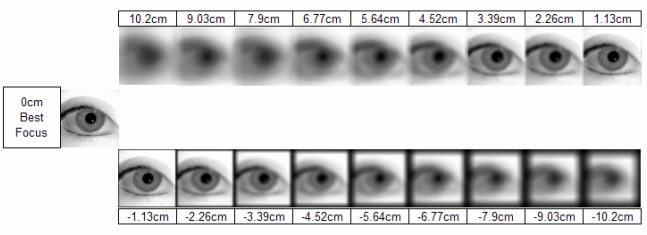

Fig. 5. Sample SIRIS simulated standard images.

[2] For information on obtaining SIRIS, contact author V.P. Pauca.

Notice that appropriate magnification of the iris due to movement away and towards the camera is taken into account.

- Wavefront encoded images (referred to hereafter as unrestored cubic): In addition to defocus blur, these images include the effect of the pupil phase mask with α=30. As before, the defocus distance ranges from -10.2 to 10.2cm from the plane of best focus. This range is the same as that used for the standard images. In this work the wavefront encoded images were not restored, i.e., no digital filter was applied to reverse the effects of the cubic phase mask. This is an important aspect of this study.

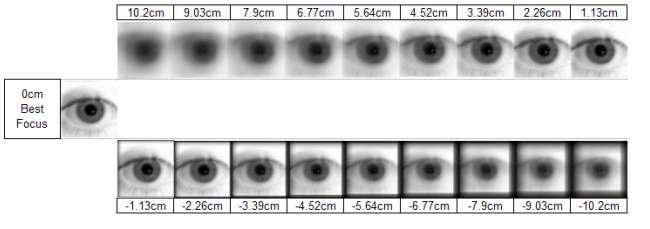

Fig. 6. Sample SIRIS unrestored cubic images.

A total of 427,500 simulated standard and wavefront encoded images were generated.

E. Processing for Iris Recognition

After simulation, the images were processed using an implementation of Daugman's algorithm [5] provided to us for research purposes by Iridian Technologies, Inc. Specifically, for a single image type (standard or unrestored cubic), we computed the Hamming distance (a) for all iris pairs at the same distance from the plane of best focus, and (b) for all iris pairs where only the reference image is at the plane of best focus. In the first case, both the verification and enrollment images[3] contain the same amount of defocus blur. In the second case (a more realistic scenario), the enrollment images do not contain defocus blur. For our dataset, this implies the computation of a total of 4x150x150x19 matching scores (~ 1.7 million comparisons).

III. Results and Analysis

The analysis reported herein includes an examination of the mean and standard deviation information of the Hamming distance results. Two matching experiments were conducted: (a) comparing standard images against standard images, and (b) comparing unrestored cubic against unrestored cubic images. These experiments correspond to two different operational scenarios where verification and enrollment images from different imaging modalities (standard vs. WFC) are not mixed. The insertion of the cubic phase mask results in a shifting of the information content in the spatial domain. Thus, the information being used to compare the images would be fundamentally different from that used in standard systems. Although the entropy of the iris image is retained, the order in the spatial domain is not. The scenario where standard and unrestored cubic images are simultaneously employed in the iris recognition process is an interesting consideration that will be explored in future work.

[3] In every matching operation, one of the images is assumed to be an "enrollment" or "reference" image while the other is referred to as the "verification" image (i.e., gallery and probe image, respectively).

A. Results

The analysis reported here represents a comprehensive comparison of matching results for all individuals within the dataset. The presented results indicate the mean Hamming distance scores and the corresponding standard deviations for both genuine and imposter data. **Fig. 7** shows the results of this analysis (users 1-50) for the first case where verification and enrollment images contain the same amount of blur.

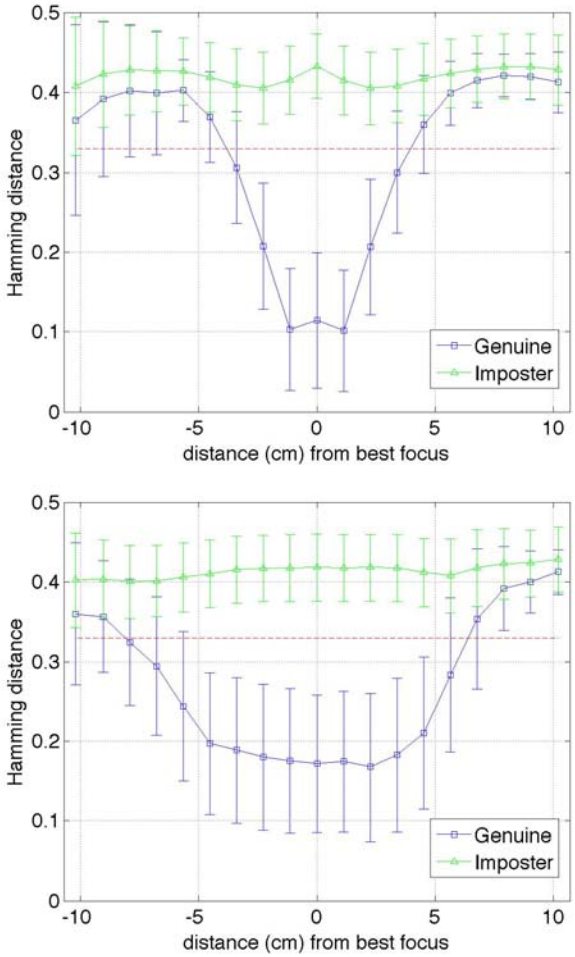

Fig. 7. Imposter and genuine score statistics of standard (above) and unrestored cubic imagery (below) where verification and enrollment images contain the same amount of blur.

The dashed line indicates the Hamming distance threshold of 0.33 observed by John Daugman in [18] (the minimum hamming distance observed among millions of imposter comparisons). In the curves corresponding to the standard images seen in **Fig. 7**, the mean of the genuine score distribution begins at a low Hamming distance at best focus but rapidly degrades as the distance from best focus increases. In comparison, the mean of the genuine score distribution for

the unrestored cubic imagery stays low over a much larger region around the plane of best focus. Table III shows the approximate average operational range for both the scenarios.

TABLE III
OPERATIONAL RANGE COMPARISON BASED ON THE SIMULATED DATA

Image Type	Distance (cm)		Operational Range (cm)
Standard	-4.2	4	~8.2
Wavefront Coded	-7.5	6	~13.5

Fig. 8 shows the results of the analysis (users 1-50) for the second case where the enrollment images do not contain defocus blur. The operational range is reported in Table IV.

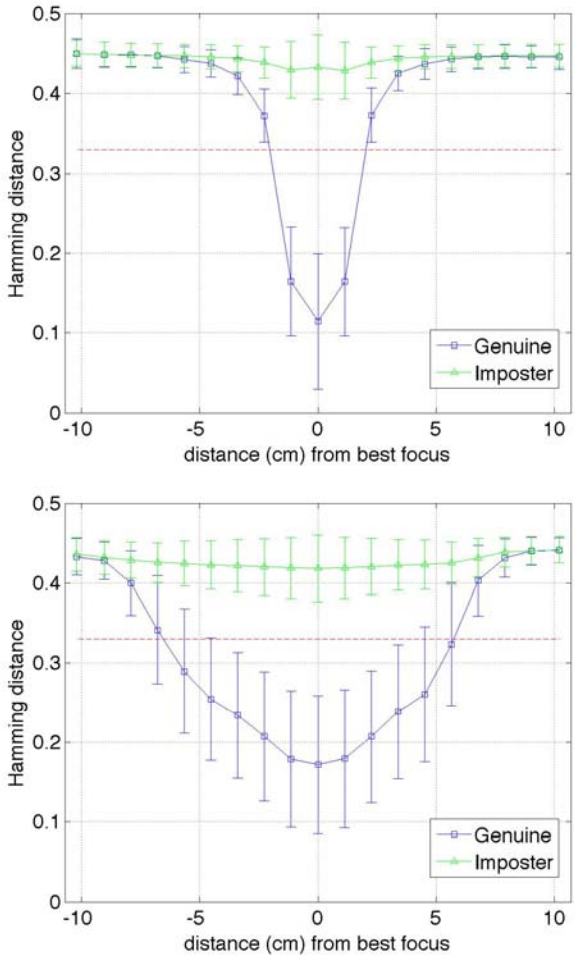

Fig. 8. Imposter and genuine score statistics of standard (above) and unrestored cubic imagery (below) in which only the enrollment images are at the plane of best focus.

TABLE IV
OPERATIONAL RANGE COMPARISON TO BEST FOCUS BASED ON THE SIMULATED DATA

Image Type	Distance (cm)		Operational Range (cm)
Standard	-2	2.5	~4.5
Wavefront Coded	-7	5.8	~12.8

As is evident in the performance noted above in Fig. 8 and Table IV, wavefront coded imaging can significantly increase the operational range of iris recognition imaging systems, even without digital restoration. These results are in accordance with results in previously published literature [5][9] and highlight the efficacy of the simulation tool in generating WFC imagery useful for research in this field.

Future work will introduce image restoration of wavefront coded imagery in the iris recognition process. We expect restored images to produce results closer to that of the standard images at 0 defocus distance, and increase the operational range of both standard and unrestored cubic imagery, at the cost of increasing the computational requirements of the imaging system.

The plots of Fig. 7 (where verification and enrollment images contain the same amount of defocus blur) show large standard deviations at points farthest from the camera (around -10.2 cm). This behavior is caused by an apparently large fluctuation in Hamming distance as the iris is "moved away" from the camera. Fig. 9 shows how the Hamming distance can decrease (for a standard system) at approximately -8cm from the plane of best focus.

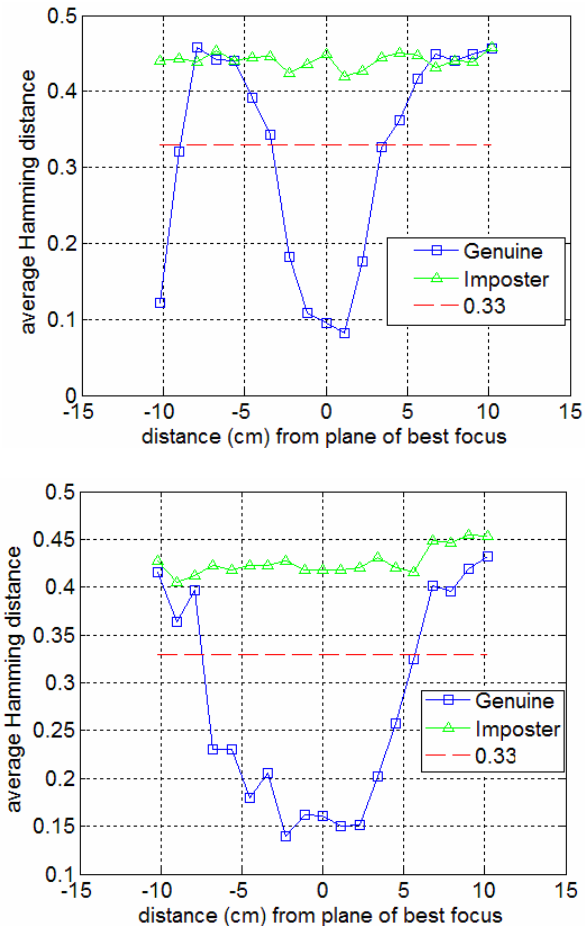

Fig. 9. The standard (above) and unrestored cubic (below) performance of a user, whose Hamming distance plot exhibits anomalous behavior.

A closer inspection of the data shows that this behavior is caused by a failure of the segmentation process as a result of scaling and excessive blur of the iris at such relatively long distances. This apparent anomaly can only be seen in a research implementation of Daugman's algorithm (such as the one used in this work), where quality control features for ensuring successful segmentation have been deliberately disabled. Table V depicts the number of users in multiple Hamming distance intervals (mean of genuine scores) at a -10.2cm depth of field. It is interesting to note the number of users whose match scores fall below the .33 Hamming distance threshold at -10.2 cm using the standard images.

TABLE V
THE DISTRIBUTION OF USERS ACROSS MULTIPLE HAMMING DISTANCE (HD) INTERVALS (DEPTH OF FIELD IS -10.2 CM). SEE FIG. 7 AND FIG. 9.

Hamming Distance Range	Standard	Unrestored Cubic
HD<.15	5	0
.15<HD<.20	3	1
.20<HD<.25	1	3
.25<HD<.30	1	5
.30<HD<.35	2	4
.35<HD	38	37

There is an important practical consideration for exploring the apparent anomaly observed in Fig. 7: while the rejection of genuine users may be tolerated at extended distances, the acceptance of imposter users should not be tolerated. Thus, image quality control will continue to be an important feature of commercially available iris recognition software.

B. Increase of Operational Range

The primary purpose of this work was (a) to extend the performance results of WFC published in the literature using a larger and statistically relevant iris dataset, and (b) to investigate the appealing prospect of extending the operational range of iris recognition without increasing the computational requirements of the system and processing time. The previously published work included a dataset size of less than ten (10) individuals [6]. The work reported in this paper is based on a dataset containing irises of fifty (50) individuals, with three (3) different input images per user, for a total of one-hundred and fifty (150) irises. As indicated by the results shown in Table VI, a consistent increase in the operational range, within the parameters allowed by the different systems, is seen between the previously published results (small dataset) and the results presented here (larger dataset). Although it is difficult to make a large scale performance claim upon a dataset of only fifty (50) users, in relation to previous work, this represents a substantial increase that helps justify the development and implementation of wavefront coded technology in the iris recognition field.

In this work, the performance of matching wavefront encoded iris images with standard iris images was not evaluated due to the distortion of spatial information content in the former. This will be a topic for future study.

TABLE VI
COMPARISON OF PERCENTAGE INCREASE IN OPERATIONAL RANGE OF DEPTH OF FIELD

Operational Range Enhancement	Standard (cm)	Unrestored Cubic (cm)	Gain
Previously published results	14	23	~1.6
This paper	4.5	12.8	~2.8

IV. CONCLUSIONS

Operational range plays a major limiting role in the application of iris recognition technology. The addition of a wavefront coding element was shown, via simulation, to significantly increase the operational range of iris recognition, even in the absence of restoration schemes. The tradeoff between degradation in Hamming distance scores and the inclusion of the cubic phase mask was also demonstrated. While the utility of the simulation software has also been anecdotally verified against actual blurred and wavefront coded imagery, an investigation on the use of wavefront coding imaging technology on a large image collection is needed.

Future initiatives would consider the development of novel pattern recognition algorithms to capitalize on the information provided by the wavefront coded element. The use of segmentation methods that are less reliant on sharp pupil/iris and iris/sclera boundaries will also help improve performance. This paper has shown that WFC technology can improve the operational range associated with iris recognition systems; this is accompanied by a reduction in SNR that does not dramatically affect the performance of the system. Additional work in systems engineering and performance optimization is necessary in order to reap the benefits of this technology.

REFERENCES

[1] R. Wildes. Iris Recognition. In Wayman et al. (Eds) Biometric Systems, Springer, London, 2005.

[2] K. Bowyer, K. Hollingsworth, and P. Flynn. "Image Understanding for Iris Biometrics: A Survey," Univ. Notre Dame CSE, Tech. Report, 2007.

[3] J. Mauldin. "Light, Lasers, and Optics" TAB BOOKS Inc. Blue Ridge Summit, Pa: 1988, Pg 46.

[4] E.R. Dowski, Jr. and W.T. Cathey, "Wavefront Coding for Detection and Estimation with a Single-Lens Incoherent Optical System," ICASSP Conference Proceedings, Vol. 4, May 1995.

[5] R. Plemmons, M. Horvath, E. Leonhardt, P. Pauca, S. Prusad, S. Robinson, H. Setty, T. Torgersen, J. van der Gracht, E. Dowski, R. Narayanswamy and P.E.X. Silveira, "Computational Imaging Systems for Iris Recognition", Proc. of SPIE Vol. 5559, August 2004.

[6] R. Narayanswamy, G.E. Johnson, P.E.X. Silveira and Hans Wach. "Extending the imaging volume for biometric iris recognition," Applied Optics, Col. 44, February 2005.

[7] S. Bradburn, E.R. Dowski, and W.T. Cathey. Realizations of focus invariance in optical-digital systems with wavefront coding. Applied Optics, 26:9157-9166, 1997.

[8] W.T. Cathey and E.R. Dowski. New paradigm for imaging systems. Applied Optics 41(29):6080-6092, 2002.

[9] E.R. Dowski, R.H. Cormack, and S.D. Sarama. Wavefront coding: Jointly optimized optical and digital imaging systems. In Proc. AeroSense Conference, Orlando, FL, April 2000.

[10] K. Kubala, E.R. Dowski, and W.T. Cathey. Reducing complexity in computational imaging systems. Optics Express, 11 (18): 2102-2108, 2003.

[11] S. Prasad, T. C. Torgersen, V.P. Pauca, R. J. Plemmons, and J. van der Gracht. High-Resolution Imaging Using Integrated Optical Systems, International Journal on Imaging Systems and Technology, Vol. 14, No. 2, pp. 67–74, 2004.

[12] S. Prasad, V.P. Pauca, R.J. Plemmons, T.C. Torgersen, and J. van der Gracht. Pupil-Phase Opti-mization for Extended-Focus Aberration-Corrected Imaging Systems, Proc. SPIE Advanced Signal Processing Algorithms, Architectures, and Implementations XIV, Vol. 5559, pp. 335–345, 2004.

[13] P.E.X. Silveira and R. Narayanswamy, "Signal-to-Noise analysis of task-based imaging systems with defocus," Applied Optics, Vol. 45, May 2006.

[14] R. Narayanswamy, P Silveira, H. Setty, V.P. Pauca, J. van der Gracht, "Extended depth-of-field iris recognition system for a workstation environment," Proc. SPIE Vol 5779, pp. 41-50, Biometric Technology for Human Identification II, May 2005.

[15] J. van der Gracht, V. Pauca, H. Setty, R. Narayanswamy, R. Plemmons, S. Prasad, and T. Torgersen. Iris recognition with enhanced depth-of-field image acquisition, Proc. SPIE Visual Information Processing XIII, vol. 5438, pp. 120–129, Orlando, FL, 2004.

[16] P. J. Phillips, W. T. Scruggs, A. J. O'Toole, P. J. Flynn, K.W. Bowyer, C. L. Schott, and M. Sharpe. "FRVT 2006 and ICE 2006 Large-Scale Results," National Institute of Standards and Technology, NISTIR 7408, http://face.nist.gov, 2007.

[17] E.N. Leonhardt and V. P. Pauca, "A User Guide for SIRIS: Simulator of Iris Recognition Imaging Systems" Wake Forest Group, August 2004.

[18] J. Daugman, "How Iris Recognition Works," IEEE Transactions On Circuits And Systems For Video Technology, Vol. 14, No. 1, January 2004.

[19] A. K. Jain, Fundamentals of digital image processing. Information and System Sciences. Prentice-Hall International, 1989.